Published in final edited form as:
Dev Biol. 2010 July 1; 343(1-2): 84–93. doi:10.1016/j.ydbio.2010.04.011.

BMP Signaling Controls Formation of a Primordial Germ Cell Niche within the Early Genital Ridges

Brian Dudley[1], **Caterina Palumbo**[2], **Jennifer Nalepka**[3], and **Kathleen Molyneaux**[1]

[1]Department of Genetics, Case Western Reserve University, Cleveland OH

[2]College of Medicine, University of Toledo, Toledo OH

[3]Athersys Inc., Cleveland OH

Abstract

Stem cells are necessary to maintain tissue homeostasis and the microenvironment (a.k.a. the niche) surrounding these cells controls their ability to self renew or differentiate. For many stem cell populations it remains unclear precisely what cells and signals comprise a niche. Here we identify a possible PGC niche in the mouse genital ridges. Conditional ablation of *Bmpr1a* was used to demonstrate that BMP signaling is required for PGC survival and migration as these cells colonize the genital ridges. Reduced BMP signaling within the genital ridges led to increased somatic cell death within the mesonephric mesenchyme. Loss of these supporting cells correlated with decreased levels of the mesonephric marker, *Pax2*, as well as a reduction in genes expressed in the coelomic epithelium including the putative PGC chemo-attractants *Kitl* and *Sdf1a*. We propose that BMP signaling promotes mesonephric cell survival within the genital ridges and that these cells support correct development of the coelomic epithelium, the target of PGC migration. Loss of BMP signaling leads to the loss of the PGC target resulting in reduced PGC numbers and disrupted PGC migration.

Keywords

mouse; primordial germ cells; bone morphogenetic proteins; Kitl; stem cells; cell migration; cell tracking

Introduction

In the adult, the tissue homeostasis and repair of multiple organ systems are controlled by resident stem cells. These stem cell populations divide slowly giving rise to new stem cells or to daughter cells that differentiate to replace tissue lost to aging or injury. The development of stem cell populations and their subsequent ability to renew or differentiate are controlled by an elaborate array of signaling interactions between the stem cells and their surrounding support cells. How these niches arise during embryogenesis is unclear but the process requires careful coordination of both stem cell and surrounding support cell development in order to insure long-term tissue homeostasis in the adult.

*Address correspondence to Kathleen Molyneaux (kam53@case.edu). 216-368-1823. Fax: 216-368-0491.

Germ cells have emerged as an ideal system to study stem cell biology (Donovan and de Miguel, 2003). Germ cells are the precursor cells of the gametes. In the mouse embryo, primordial germ cells (PGCs) are induced to form within the posterior proximal epiblast between day 6.5 and 7.5 (E6.5-E7.5) of gestation. Once formed, PGCs migrate through the posterior primitive streak and become incorporated into the invaginating hindgut (Anderson et al., 2000). PGCs remain in the hindgut until E9.5 when they actively migrate through the body wall, dorsally, then laterally to colonize the genital ridges (Molyneaux et al., 2001). At the ridges PGCs associate with the somatic support cells that will either direct their fate towards becoming the self-renewing stem population in the testis, or the non-renewing oocyte pool within the ovary.

Being motile, PGCs occupy many different niche environments prior to colonizing the gonads. For example, the posterior proximal epiblast (PPE) has been dubbed an embryonic germ cell niche (Saitou et al., 2002). PGCs arise in this region in response to multiple BMP family members. First, BMP8b is required to control the anterior-posterior patterning of the visceral endoderm thereby allowing for establishment of a permissive region within the PPE. Cells in the PPE then respond either directly (Ohinata et al., 2009) or indirectly (de Sousa Lopes et al., 2004) to additional BMP family members that induce them to become PGCs.

Additional growth factors and adhesive interactions are required to control PGC migration, proliferation and survival as they migrate to colonize the genital ridges (Molyneaux et al., 2004). The growth factors KITL (Wehrle-Haller and Weston, 1995) and SDF1a (Stebler et al., 2004) are expressed in the hindgut and later in the genital ridges. KITL (Bennett, 1956; Mahakali Zama et al., 2005; Runyan et al., 2006; Russell, 1979) and SDF1a (Ara et al., 2003) are critical for controlling PGC numbers and may direct PGC migration. However, precisely how the somatic cells along the migration route coordinate expression of these factors remains uncertain and in many cases, even the identity of the supporting cells themselves is unclear.

This study provides evidence that PGC development is coupled to differentiation of the mesonephros and that both systems rely on BMP signaling. In a previous study, an organ culture system was used to demonstrate that BMP signaling regulates expression of *Kitl* within the nascent genital ridges (Dudley et al., 2007). In this study, conditional gene targeting was used to confirm the role of BMP signaling during PGC migration in vivo. Additionally, we demonstrate that BMP signaling controls cell survival and possibly cell identity within the genital ridges. We propose that this represents an early and probably transient PGC niche that is established in the genital ridges prior to differentiation of the sertoli or granulosa cell support lineages.

Methods

Mice and tamoxifen injections

The Case Western Institutional Animal Care and Use Committee approved all experiments involving mice. *Bmpr1a-fx* mice provided by Y. Mishina were crossed with Oct4ΔPE:GFP mice (Anderson et al., 1999) and Rosa:LacZ mice (Soriano, 1999), and all three loci were bred to homozygosity. Mice carrying the *CAGGCre-ER*™ transgene (Hayashi and McMahon, 2002) or *Pax2-Cre* (Ohyama and Groves, 2004) were crossed to mice carrying the *Bmpr1a* null allele *Bmpr-s* (Mishina et al., 1995). Male *Bmpr1a-fx/Bmpr1a-fx Oct4ΔPE:GFP/Oct4ΔPE:GFP Rosa:LacZ/Rosa:LacZ mice* were crossed with *CAGGCre-ER*™/+ *Bmpr-s*/+females resulting in four different genotypes (Figure 1H). Noon on the day that a vaginal plug was detected was considered E0.5. E8.5 pregnant females were weighed and treated with tamoxifen via oral gavage (9mg TM in corn oil per 40g body weight) (Hayashi and McMahon, 2002). Embryos were then harvested 24, 36, or 48 hours later.

PGC counts and immunohistochemistry

For PGC counts, embryos were harvested at E10.5 and transverse sections between the fore- and hind-limb buds were cut by hand. Optical sections of tissue slices were collected at 5 μm intervals using a Leica TCS AOBS filter-free Confocal Laser Scanning microscope. Images were processed using Volocity software and the numbers of PGCs were counted. For each slice, the number of PGCs per 100 μm was calculated (n = number of PGCs per slice / slice thickness * 100 μm). Counts were normalized to the average wild type value for each litter in order to minimize the effect of variations in age between litters. E9.5 PGC counts were obtained by analyzing images from time-lapse experiments.

Immunostaining of dissected tissue slices was performed using pSMAD1/5/8 antibodies (Cell Signaling Technology) or cleaved PARP antibodies (Cell Signaling Technology). For pSMAD1/5/8 staining, embryos were fixed in 8% PFA/PBS overnight at 4°C. Transverse sections were then cut by hand and slices were dehydrated through a methanol series. Slices were then rehydrated through the MeOH series and further permeabilized by treatment in PBS/0.1%TX-100 (PBTX) for at least 2 hours. Slices were then blocked in 2% goat serum and 2% IgG-free BSA in PBTX (goat block) overnight at 4°C. Then, slices were incubated with rabbit-anti-pSMAD1/5/8 diluted 100 fold in goat block, overnight at 4°C. The slices were rinsed 5 times, one hour each, in PBTX at room temperature. Slices were then exposed to goat-anti-rabbit IgG Cy5 secondary antibodies (Jackson Immunoresearch Laboratories, Inc.) diluted 100 fold in goat block overnight at 4°C. The tissue was then rinsed 5 times, one hour each, in PBTX. Slices were stored in 1:4 PBS:Glycerol before collecting confocal images. Volocity software was used to process the images and to measure pixel intensity. Cleaved PARP antibody staining followed the same protocol as above except that slices were fixed in 4% PFA/PBS and were not taken into MeOH. The rabbit anti-cPARP antibody was diluted to 1:250 in goat block, and the secondary goat-anti-rabbit IgG cy5 was diluted to 1:200. Frozen sections were used for β-gal antibody staining. Briefly whole embryos were fixed in 4% PFA/PBS overnight at 4°C, rinsed in PBS and PBTX, and then rinsed three times for 30 minutes each in O.C.T. compound (Sakura Finetek). Embryos in O.C.T. were then transferred to plastic blocks and frozen. Sections were cut to a thickness of 14 μm and stored at −20°C. Slides were rinsed twice in 1X PBS and once in PBT (0.25% Triton X-100, 1X PBS) for 5 minutes each. The tissue was then blocked with 10% donkey serum in PBT (donkey block) for 1 hour at RT then incubated overnight in 1:250 β-gal antibody (Biogenesis, Inc.) in donkey block at 4°C. Slides were rinsed 5 times for 10 minutes each in PBT and then exposed to 1:100 donkey-anti-goat IgG (H+L) Alexa Flour 555 (Molecular Probes) in 1% donkey serum in PBT for 1 hour at RT. Slides were rinsed 5 times for 10 minutes each in PBT and mounted in Vectashield with DAPI (Vector Laboratories, Inc.) overnight at 4°C. Staining was imaged on a Leica DM6000B microscope and images were processed using Volocity software. Whole embryos were stained with X-gal as described (Hogan, 1994).

pSMAD1/5/8 staining was measured using Volocity. pSMAD1/5/8 Pixel intensity throughout all z-planes of the image was divided by the volume of the measured image yielding the intensity per volume. Measurements were normalized to the average pixel intensity per volume of the wild type samples.

Cleaved PARP foci were counted in Volocity by selecting the mesonephric mesenchyme, coelomic epithelium, and boundary of the hindgut using the region of interest (ROI) tool. Positive foci were identified by detecting the top 30 – 100% intensity on the Cy5 channel. Foci were restricted to the ROI using the “Clip to the ROI” command. Objects greater than 1000 μm^3 were separated (reflecting the fact that clusters bigger than 1000 um^3 usually represented multiple touching foci instead of a single foci). Objects less than 100 μm^3 were excluded. Objects matching these parameters were counted by the software, the volume of the ROI was recorded, and counts were normalized to the average volume for each region.

Gene expression analysis

Changes in gene expression were monitored by quantitative real time PCR (q-RT-PCR). Briefly, E10.5 embryos were harvested and either tissue slices or genital ridges were dissected as described (Dudley et al. 2007). Total RNA was isolated by homogenizing tissue in 300 µl of TriZOL (Invitrogen) in the presence of 5 µg linear polyacrylamide (Sigma-Aldrich Co.). Isolated RNA was treated with RQ1 DNase (Promega). cDNA was synthesized using the SuperScript III First Strand cDNA Synthesis Kit with oligo dT priming (Invitrogen). A minimum of 15 ng of template RNA was used per 10 µl cDNA reaction. An RT- negative control was run for each experiment to monitor the effectiveness of the DNase treatment by having one sample run without the SuperScript III reverse transcriptase. Following the RT reaction, samples were diluted 10 fold with nuclease-free water. qPCR was run using the Brilliant II SYBR Green Master Mix (Promega) and primers for *Bmpr1a, Kitl, Pax2, Id1, Sdf1a, Scarb1* and the loading controls *bAct* and *Tbf* (Supplemental Table 1). Raw data was normalized according to the average of *bAct* and *Tbf* for each sample. For each litter, values were then expressed as a percent relative to the average wild type, allowing for comparisons among litters.

Time-lapse

Tissue dissection and filming was conducted as previously described with some modifications (Molyneaux et al., 2003). Briefly E8.5 pregnant females were exposed to TM as described above and E9.5 embryos were harvested. Transverse sections were then cultured as described and a single optical section was captured every 7 minutes for approximately 11.8 hours (100 frames). Cell traces were generated using the automated tracking feature of Volocity software. First, noise was removed from the GFP channel. Cells were identified based on intensity (top 40% of the GFP channel). Holes were filled in the identified objects. Touching cells were separated based on a size threshold of 100 μm^2. Objects less than 40 μm^2 and larger than 300 μm^2 were excluded. Tracking was then performed using the "Shortest Path" algorithm with a maximum distance between nodes of 10 µm. Targeting and average velocity measurements were calculated from 20 traces with the highest trace times, excluding any traces with times less than one hour. PGC targeting was measured by connecting a PGC's start point and end point with a straight line then extrapolating that through the tissue in the direction the PGC was moving. If the line intersected a genital ridge, it was recorded as targeting (Figure S3).

Statistics

Gene expression values, pSMAD1/5/8 levels, cleaved PARP staining, PGC counts and tracking data were compared between the four different genotypes using one-way ANOVA. Following analysis of variance, between group differences were determined using the Fisher's least significant difference post test. Calculations were performed in Excel.

Results

BMP signaling components are expressed in the genital ridges during PGC migration

BMP signaling components are present and active in the genital ridges as PGCs migrate to and colonize this region. E9.5 and E10.5 embryos were harvested and transverse sections between the fore- and hind-limb buds were isolated (Figure 1A). In situ hybridization data show that at least two BMP ligands are expressed in the genital ridges at E9.5 and E10.5. *Bmp4* expression was detected in the mesonephric mesenchyme at E9.5 with lower expression in the midline dorsal to the hindgut (Figure 1B). BMP4 expression was elevated in the posterior end of the embryo encompassing the tail bud and the remnant of membrane surrounding the umbilical vein. By E10.5 *Bmp4* expression remained high in the mesonephros (data not shown) with additional regions corresponding to known domains of BMP4 expression including the dorsal margin of the eye (Furuta and Hogan, 1998), the outflow tract of the heart (Jiao et al., 2003),

the limb buds (Hogan et al., 1994) and the dermomyotome of the developing somites (McMahon et al., 1998). At E12.5 *Bmp4* continued to be expressed in the gonads as well as the developing kidneys (data not shown). *Bmp7* was also expressed in the developing urogenital system. At E9.5 *Bmp7* was observed in the mesonephric duct of the genital ridges (Figure 1C). By E10.5 expression had expanded to include the somites, the limb buds (Zakin et al., 2005), and the myocardium of the heart (Solloway and Robertson, 1999) (data not shown). In the E12.5 urogenital system, *Bmp7* expression was found in the kidneys (Dudley and Robertson, 1997) and in the sex cords of the developing testis (Ross et al., 2007) (data not shown). *Bmp2* expression was not detected at E9.5 or E10.5 in the genital ridges but signals were seen in known domains of BMP2 expression including the outflow tract of the heart (Christoffels et al., 2004) and the ventral margin of the limb bud (Moon et al., 2000) (data not shown). At E12.5 *Bmp2* expression was observed in the developing kidneys (Dudley and Robertson, 1997) and weakly in the gonads (data not shown).

To determine which cell populations respond to endogenous BMPs, we performed immunostaining with an antibody that recognizes phosphorylated SMAD1/5/8. Staining of E9.5 transverse sections showed activated SMADs at low levels throughout most of the section (Figure 1D) (Dudley et al, 2007). Staining was most intense in the mesonephric mesenchyme and coelemic epithelium of the genital ridges. Bright staining was also observed in the dorsal neural tube and in the dermomyotome of the somites. At E10.5, pSMAD1/5/8 staining was no longer elevated in the coelomic epithelium but remained strong in the mesonephric mesenchyme and in the dorsal neural tube, with low levels throughout the slice (Dudley et al, 2007) (Figure 1E).

Conditional loss of Bmpr1a leads to decreased BMP signaling

To target BMP signaling in vivo we used a ubiquitously expressed *CreER* transgene, CAGGCre-ER™ (Hayashi and McMahon, 2002), to knock out a conditional allele of *Bmpr1a* (Mishina et al., 2002) (Figure 1F). *Bmpr1a* encodes for one of three type one BMP receptors in the mouse and is the preferred receptor for BMP4 (ten Dijke et al., 2003), the ligand that appeared to be the most abundantly expressed in and along the PGC migration route (Figure 1B). First, we tested excision efficiency of the CAGGCre-ER™ line, hereafter referred to as "CreER." *CreER/+* mice were crossed to a *Rosa:LacZ* reporter line. E8.5 pregnant females were injected with tamoxifen and embryos were harvested at E9.5 and either stained for β-gal activity as whole mounts (data not shown) or cryosectioned to examine β-gal expression via immunostaining. Immunostaining with an antibody directed against β-gal showed moderate recombination throughout the entire section (Figure 1G). A breeding schema was established to allow for inducible recombination of one conditional allele over a null allele, *Bmpr-s* (Mishina et al., 1995), to increase efficiency of knockdown (Figure 1H). Quantitative real-time PCR was then used to monitor the efficiency of *Bmpr1a-fx* recombination in tissue slices dissected from between the fore- and hind-limb buds (Figure 2). Primers were designed to detect only full length *Bmpr1a* cDNA (Figure 1F, arrows). In the absence of TM, wild type (WT) samples expressed *Bmpr1a* at an average normalized level of 95.5 ± 4.5%, conditional heterozygotes (C-Het) at 76.8 ± 6.1%, *Bmpr-s* heterozygotes (B-Het) at 50.0 ± 6.2%, and conditional knock outs (KO) at 49.5% (Figure 2A). Administration of TM to E8.5 pregnant females resulted in near complete loss of *Bmpr1a* expression in KO embryos by E10.5 (Figure 2B). Average normalized WT *Bmpr1a* expression was found to be 104.9 ± 8.9%, compared to C-Het expression at 65.8 ± 5.9%, B-Het at 57.2 ± 7.6%, and KO at 5.2 ± 3.0%. This experiment was repeated while varying the length of time embryos were exposed to TM in utero. Recombination was detected as early as 6 hours after TM exposure (Figure S1). Within 12 hours average expression in KOs was 18% of WT littermates.

To confirm that a reduction in *Bmpr1a* expression leads to decreased BMP signaling in vivo, TM exposed embryos were fixed and stained with an antibody directed against phosphorylated SMAD1/5/8 (Figure 2C–F). Embryos exposed to TM at E8.5 showed no change in pSMAD1/5/8 levels by E9.5 (Figure 2C, C', and E). However, by E10.5, KO embryos had greatly reduced pSMAD1/5/8 staining (Figures 2D, D', and F). Remaining E10.5 pSMAD1/5/8 activity could be attributed to incomplete turnover of endogenous BMPR1a or the activity of other Type I BMP receptors.

The Cre-ER transgene is effective at reducing *Bmpr1a* mRNA levels and BMP signaling in the entire trunk of the E10.5 embryo. However, to more precisely target BMP signaling within the genital ridges, we attempted tissue specific targeting utilizing the Pax2-Cre line developed by Ohyama and Groves (2004). *Pax2* is a transcription factor required for kidney development. It is expressed in the pronephros at E9.0 and in the mesonephric duct and adjacent mesonephric mesenchyme at E10.5 (Xu et al., 2003). We demonstrate that Pax2-Cre can induce recombination of a LacZ reporter within the mesonephric duct and anterior mesonephric mesenchyme by E9.5 (Figure S2A). Additionally, *Bmpr1a* mRNA levels are reduced in genital ridges isolated from *Pax2-Cre/+ Bmpr1a-fx/Bmpr1a-s* E10.5 animals (Figure S2B). However, pSMAD1/5/8 levels remained high in genital ridges from these animals (Figure S2C) and there was no significant effect on PGC numbers (Figure S2D). This indicates that this driver line may not recombine early enough or efficiently enough to reduce BMPR1a protein levels and impact signaling during PGC migration. Therefore, we discontinued the use of this line and focused our analysis on the CreER crosses.

Decreased Bmpr1a expression correlates with changes in BMP target gene expression

We have previously shown that in culture BMP signaling controls the expression of target genes within the genital ridges as PGCs migrate to colonize these structures (Dudley et al., 2007). To test if BMP signals control genital ridge gene expression in vivo, we used real time PCR to compare the expression of ridge marker genes in induced knock out animals and their littermates. In the chick, *Pax2* expression within the lateral plate is controlled by BMP signaling (Obara-Ishihara et al., 1999). The growth factor *Kitl* is a BMP responsive gene (Dudley et al., 2007; Otsuka and Shimasaki, 2002) required for PGC survival and potentially motility. *Kitl* is expressed along the migratory route of PGCs and its expression increases within the E10.5 genital ridges as PGCs colonize these structures (Dudley et al., 2007; Keshet et al., 1991). To detect tissue specific changes in target gene expression, transverse tissue pieces were dissected to separate genital ridge tissue from neural tube (NT) and gut tissue as previously described (Dudley et al., 2007). *Bmpr1a* expression in KO tissue was reduced to 23.8 ± 3.8% in the genital ridges (Figure 3A). Expression of the known BMP target gene *Id1* (Valdimarsdottir et al., 2002) was reduced to 55.0 ± 6.1% in KO genital ridges relative to WT littermates (Figure 3B). Genital ridge expression of *Kitl* in KO embryos was reduced to 35.3 ± 4.9% that of the wild type (Figure 3C). *Pax2* expression in KO embryos was reduced to 46.3 ± 7.0% in the genital ridges (Figure 3D). Expression of *Sdf1a*, a putative PGC chemoattractant expressed in the genital ridges (Molyneaux et al., 2003), was reduced in C-Het and KO genital ridges relative to WT (Figure 3E). While some mesenchymal (*Pax2*) and epithelial (*Sdf1a* and *Kitl*) marker genes were down regulated in response to decreased BMP signaling, the expression of *Scarb1*, an epithelial marker in the ridge, was slightly up regulated in KO genital ridges relative to wild type and heterozygous littermates (Figure 3F).

Reduced BMP signaling leads to decreased targeting of PGCs to the genital ridges

Decreased BMP signaling in KO embryos led to reduced expression of *Kitl* and *Sdf1a* (Figure 3), two factors that have been shown to be involved in PGC migration at this stage. This suggested that there might be migration defects in the *Bmpr1a* conditional KO embryos. To monitor PGC migration we used confocal time-lapse microscopy. At E9.5, WT PGCs are

located near the midline then migrate laterally to colonize the genital ridges over the next 24 hours (Movie 1, 11 hours shown). However, in KO samples, fewer PGCs migrate towards the genital ridges (Movie 2). To quantify the migration defects in the KO embryos we used Volocity software to track PGCs (Figure 4). PGC tracks were then scored as either targeting the nearest genital ridge or an ectopic region (Figure S3). While only 60% of PGCs in WT embryos were observed targeting the nearest genital ridge, approximately 43% of PGCs in KO embryos were observed targeting the nearest genital ridge (Figure 4A–C). There was no significant difference in the average length of time that the software was able to track a PGC in WT, heterozygous, and KO PGCs (Figure S4). Similar trace times suggest that the observed differences in PGC targeting are not artifacts of the variation in the ability of the program to follow PGCs for their entire migration. In addition to decreased PGC targeting, KO PGCs had a slightly lower average velocity than WT PGCs (Figure 4D).

Conditional Bmpr1a knock out embryos have fewer migratory PGCs

We have previously shown that migratory PGCs are sensitive to BMP levels in organ culture. In this study we monitored the effect of decreased BMP signaling on migratory PGCs in vivo (Figure 5). Embryos were exposed to TM at E8.5 and harvested at E9.5 or E10.5. There was no significant difference in the number of PGCs in E9.5 KO embryos relative to WT and heterozygous littermates (Figure S5). This is not surprising considering that 24 hours was insufficient time to allow for a reduction in pSMAD1/5/8 levels (Figure 2E). However, by E10.5, KO embryos exhibited a significant reduction in PGCs when compared to their littermates (Figure 5). Additionally the few remaining PGCs in KO embryos were often located outside of the genital ridges in the gut or midline (Figure 5D). Volocity software was used to count the number of PGCs per 100 μm of tissue. To account for stage variability between litters, PGC counts were normalized to the average number of PGCs per wild type embryo for each litter. E10.5 KO embryos were found to have significantly fewer PGCs on average than their WT littermates (38.1 ± 9.2% compared to 100 ± 4.6%) (Figure 5E). There was no significant difference between the WT embryos and either the C-Hets or B-Hets. However, C-Het embryos had significantly more PGCs than B-Het embryos, 117.6 ± 9.9% compared to 92.0 ± 7.1 % respectively.

Knock out embryos have increased genital ridge somatic cell death

The reduction in PGCs in KO embryos could be due to apoptosis, decreased proliferation, or loss of expression of the Oct4ΔPE:GFP marker should PGCs loose pluripotency. To determine if the loss of PGCs in KO embryos was due to apoptosis we fixed and stained transverse sections with a cleaved-PARP specific antibody. Following TM exposure at E8.5, there was an increase in the number of apoptotic foci in the somatic tissue of the KO embryos relative to their WT littermates (Figure 6). However, few PGCs were observed undergoing apoptosis. In E9.5 KO embryos there was scattered cell death throughout the slice with an increased concentration of apoptotic cells in the mesonephric mesenchyme of the genital ridges (Figure 6A, A', B, B' and C). Death in the mesonephric mesenchyme was more dramatic at anterior positions (compare Figure 6B and B'). On average, the mesonephric mesenchyme of WT slices had 2.0 ± 0.61 apoptotic foci per 600,000 μm^3, compared to 6.6 ± 0.88 apoptotic foci per 600,000 μm^3 in the KO mesonephric mesenchyme (Figure 6C). Increased cell death in the mesonephric mesencyhme was also observed in E10.0 genital ridges (Figures 6D, E, F, G and H). Wild type E10.0 slices had moderate levels of cell death throughout the slice (Figure 6D). However, significantly greater cell death was observed in the mesonephric mesenchyme of KO slices than of WT slices, 3.1 ± 1.2 compared to 0.72 ± 0.41 apoptotic foci per 900,000 μm^3 respectively (Figure 6H). In two KO embryos out of three litters, massive cell death was observed in the genital ridges in such density that the number of apoptotic foci could not be counted (Figure 6G) and therefore were omitted from these comparisons (Figure 6H). E10.0 B-Het embryos were found to have slightly increased numbers of apoptotic foci in the

mesonephric mesenchyme at 1.7 ± 0.19 per 900,000 μm^3, though these counts were not significantly different than the WT (Figure 6E, H). In addition to the mesonephric mesenchyme, apoptotic foci were also counted in the coelomic epithelium and the gut, however, there were no significant differences in these data sets (data not shown).

Discussion

In this study, the role of BMP signaling in PGC migration was tested by using conditional targeting to reduce BMPR1a levels. Decreased BMP signaling, as monitored by pSMAD1/5/8 levels, resulted in fewer PGCs at E10.5 and reduced targeting of migratory PGCs. This phenotype coincided with an increase in somatic cell death within the mesonephric mesenchyme of the conditional knock out genital ridges. Consistent with the high degree of apoptosis in the mesenchyme, the transcription factor *Pax2* was observed to be reduced in the KO genital ridges. Additionally expression of genes considered to be markers of the coelomic epithelial (a.k.a. pre-gonadal) compartment were also affected. Expression of the PGC survival factor *Kitl* was reduced and expression of the PGC attractant *Sdf1a* was also reduced. Expression of the epithelial marker *Scarb1* was increased. Our data demonstrates that BMP signaling is required for survival of the mesenchymal component of the genital ridge and that it may regulate cell fate decisions within the coelomic epithelial compartment of the ridge. In this manner BMP signals establish a favorable environment for arriving PGCs.

BMPs are known to be required for PGC development at various stages. Specification of PGCs in early post-implantation mouse embryos requires extraembryonic ectoderm derived BMP4 (Lawson et al., 1999) and BMP8b (Ying et al., 2001) and endoderm derived BMP2 (Ying and Zhao, 2001). These various BMP family members may act directly or indirectly to specify PGCs. In support of an indirect mechanism, de Sousa Lopes et al. (2004) have shown that the PGC deficiency in *Bmp4*$^{-/-}$ embryos can be rescued by constitutive activation of the type I BMP receptor Activin A Receptor, type 1 (ACVR1) in the visceral endoderm, but not the epiblast where PGC precursors reside. Conversely, there is evidence to suggest that BMPs directly regulate PGC specification. Ohinata et al. (2009) showed that extraembryonic ectoderm derived BMP4 can drive expression of *Blimp1* in epiblast cells, signaling directly through PGC expressed BMPR1a, as well as SMAD1 and SMAD5. The effect of BMP4 is dose dependent such that those cells that are closest to the source, and are exposed to the highest concentration, will express *Blimp1* and ultimately become PGCs. BMP4 has also been found to be necessary to differentiate PGCs from embryonic stem (ES) cells in culture (Wei et al., 2008), which may indicate a direct requirement of BMP4 in PGC specification. However, the authors noted that BMP4 can promote the formation of extraembryonic mesoderm and that PGCs may be developing within a microenvironment in an indirect way. Our data indicates that BMP signaling also acts within the nascent genital ridges to establish a supportive microenvironment for arriving PGCs. Loss of BMP signaling results in death of mesenchymal cells and reduces expression of the epithelial markers *Kitl* and *Sdf1a*. We cannot currently rule out a direct interaction between ridge expressed BMPs and arriving PGCs. Migratory PGCs express multiple BMP receptors and SMADs and are capable of responding to high levels of exogenously added BMPs (Dudley et al., 2007). However, we were unable to detect pSMAD within PGCs under normal conditions using either immunostaining or a BRE:lacZ reporter mouse (data not shown, Monteiro et al., 2004). Either migratory PGCs use non-SMAD pathways to respond to BMPs or the requirement for BMP signaling during PGC migration is entirely indirect.

Our data indicates that BMP signaling is necessary for the survival of the mesonephric mesenchyme and for PGC migration. This is the first study to couple early kidney development with PGC migration in mammals. There is evidence in zebrafish that pronephric cells of the lateral plate mesoderm are an intermediate target of migrating PGCs and disruption of this

target tissue ultimately leads to decreased PGC accumulation within the genital ridges (Weidinger et al., 2002). However, multiple previous studies in mice have suggested that PGC migration is independent of both kidney development and specification of the somatic support cells of the gonads. Mice homozygous for a null mutation in *Wilms tumor 1* (*Wt1*) exhibit increased apoptosis in the E11.0 metanephric blastema and ultimately a complete degeneration of the kidney precursor population by E12.0 (Kreidberg et al., 1993). Regardless, PGCs were observed in the E12.0 genital ridge. Additionally, mice mutant for *steroidogenic factor 1* (*Sf1*) (Luo et al., 1994) and the LIM homeobox gene *Lhx9* (Birk et al., 2000) fail to form gonads, with defects beginning by E12.0. PGCs were observed in the genital ridges at E10.5 in *Sf1* null embryos and at E12.0 in *Lhx9* null embryos. Together these data would imply that neither the developing kidney nor the gonad is necessary for proper PGC targeting and colonization of the genital ridges. However, these mutations resulted in phenotypes later than those observed in conditional targeting of *Bmpr1a*. In our conditional knock out embryos, we observed increased cell death at E9.5 within the mesonephric mesenchyme. This precedes the mutant phenotypes of the *Wt1*, *Sf1*, and *Lhx9* mutants, and results in a rapid loss of mesenchymal cells, as evidenced by increased apoptotic foci at E10.0. This increase in cell death correlates with decreased PGC survival and targeting suggesting that the requirement for mesonpehric cells occurs at least from E9.5 to E10.5.

Taken together our results indicate that BMP signaling within the mouse genital ridges during PGC migration acts to establish a permissive environment for arriving PGCs. This niche is comprised of several cell populations. The *Pax2* expressing cells of the pronephric mesenchyme both produce and respond to BMPs, including BMP4, which acts to promote their survival. Conversely, the cells of the coelomic epithelium do not rely on BMPs for survival but require it to maintain *Kitl* and *Sdf1a* expression and repress *Scarb1*. Others have shown that during early kidney development, BMP signaling in the lateral plate mesoderm drives pronephric fate while restricting hematopoietic and vascular cell fates (Bracken et al., 2008; Gupta et al., 2006; Wang et al., 2009; Winnier et al., 1995). Our data suggests that BMP signaling may promote similar cell fate choices in the coelomic epithelium, the compartment that will later give rise to the somatic components of the gonads.

In summary, BMP signaling is necessary for PGC migration, cell survival and gene expression within the genital ridges. Future experiments will attempt to dissect the role of BMP signaling in distinct cell populations within the ridge. Ultimately this analysis will provide insight into how the germ cell niche is established. It should also reveal how cell fate decisions are coordinated to give rise to distinct kidney and gonadal cell populations.

Supplementary Material

Refer to Web version on PubMed Central for supplementary material.

Acknowledgments

The BMPR-fx and BMPR-s mouse lines were generously provided by Yuji Mishina. The Pax2-Cre line was provided by Andy Groves. We thank Patti Conrad for microscopy assistance and acknowledge the use of the Leica widefield and confocal microscopes in the Genetics Department Imaging Facility at Case Western Reserve University, funded by the National Center for Research Resources (NIH-NCRR) Shared Instrumentation Grant program (1S10RR021228 and 1S10RR017980). Financial support for this work was provided by Case Western Reserve University and the NIH (R01HD053900 awarded to KM).

References

Anderson R, Copeland TK, Scholer H, Heasman J, Wylie C. The onset of germ cell migration in the mouse embryo. Mech Dev 2000;91:61–68. [PubMed: 10704831]

Anderson R, Fassler R, Georges-Labouesse E, Hynes RO, Bader BL, Kreidberg JA, Schaible K, Heasman J, Wylie C. Mouse primordial germ cells lacking beta1 integrins enter the germline but fail to migrate normally to the gonads. Development 1999;126:1655–1664. [PubMed: 10079228]

Ara T, Nakamura Y, Egawa T, Sugiyama T, Abe K, Kishimoto T, Matsui Y, Nagasawa T. Impaired colonization of the gonads by primordial germ cells in mice lacking a chemokine, stromal cell-derived factor-1 (SDF-1). Proc Natl Acad Sci U S A 2003;100:5319–5323. [PubMed: 12684531]

Bennett D. Developmental analysis of a mutation with pleiotropic effects in the mouse. Journal of Morphology 1956;98:199–233.

Birk OS, Casiano DE, Wassif CA, Cogliati T, Zhao L, Zhao Y, Grinberg A, Huang S, Kreidberg JA, Parker KL, Porter FD, Westphal H. The LIM homeobox gene Lhx9 is essential for mouse gonad formation. Nature 2000;403:909–913. [PubMed: 10706291]

Bracken CM, Mizeracka K, McLaughlin KA. Patterning the embryonic kidney: BMP signaling mediates the differentiation of the pronephric tubules and duct in Xenopus laevis. Dev Dyn 2008;237:132–144. [PubMed: 18069689]

Christoffels VM, Hoogaars WM, Tessari A, Clout DE, Moorman AF, Campione M. T-box transcription factor Tbx2 represses differentiation and formation of the cardiac chambers. Dev Dyn 2004;229:763–770. [PubMed: 15042700]

de Sousa Lopes SM, Roelen BA, Monteiro RM, Emmens R, Lin HY, Li E, Lawson KA, Mummery CL. BMP signaling mediated by ALK2 in the visceral endoderm is necessary for the generation of primordial germ cells in the mouse embryo. Genes Dev 2004;18:1838–1849. [PubMed: 15289457]

Donovan PJ, de Miguel MP. Turning germ cells into stem cells. Curr Opin Genet Dev 2003;13:463–471. [PubMed: 14550410]

Dudley AT, Robertson EJ. Overlapping expression domains of bone morphogenetic protein family members potentially account for limited tissue defects in BMP7 deficient embryos. Dev Dyn 1997;208:349–362. [PubMed: 9056639]

Dudley BM, Runyan C, Takeuchi Y, Schaible K, Molyneaux K. BMP signaling regulates PGC numbers and motility in organ culture. Mech Dev 2007;124:68–77. [PubMed: 17112707]

Furuta Y, Hogan BL. BMP4 is essential for lens induction in the mouse embryo. Genes Dev 1998;12:3764–3775. [PubMed: 9851982]

Gupta S, Zhu H, Zon LI, Evans T. BMP signaling restricts hemato-vascular development from lateral mesoderm during somitogenesis. Development 2006;133:2177–2187. [PubMed: 16672337]

Hayashi S, McMahon AP. Efficient recombination in diverse tissues by a tamoxifen-inducible form of Cre: a tool for temporally regulated gene activation/inactivation in the mouse. Dev Biol 2002;244:305–318. [PubMed: 11944939]

Hogan, B. Manipulating the mouse embryo: a laboratory manual. Plainview, N.Y.: Cold Spring Harbor Laboratory Press; 1994.

Hogan BL, Blessing M, Winnier GE, Suzuki N, Jones CM. Growth factors in development: the role of TGF-beta related polypeptide signalling molecules in embryogenesis. Dev Suppl 1994:53–60. [PubMed: 7579524]

Jiao K, Kulessa H, Tompkins K, Zhou Y, Batts L, Baldwin HS, Hogan BL. An essential role of Bmp4 in the atrioventricular septation of the mouse heart. Genes Dev 2003;17:2362–2367. [PubMed: 12975322]

Keshet E, Lyman SD, Williams DE, Anderson DM, Jenkins NA, Copeland NG, Parada LF. Embryonic RNA expression patterns of the c-kit receptor and its cognate ligand suggest multiple functional roles in mouse development. EMBO J 1991;10:2425–2435. [PubMed: 1714375]

Kreidberg JA, Sariola H, Loring JM, Maeda M, Pelletier J, Housman D, Jaenisch R. WT-1 is required for early kidney development. Cell 1993;74:679–691. [PubMed: 8395349]

Lawson KA, Dunn NR, Roelen BA, Zeinstra LM, Davis AM, Wright CV, Korving JP, Hogan BL. Bmp4 is required for the generation of primordial germ cells in the mouse embryo. Genes Dev 1999;13:424–436. [PubMed: 10049358]

Luo X, Ikeda Y, Parker KL. A cell-specific nuclear receptor is essential for adrenal and gonadal development and sexual differentiation. Cell 1994;77:481–490. [PubMed: 8187173]

Mahakali Zama A, Hudson FP 3rd, Bedell MA. Analysis of hypomorphic KitlSl mutants suggests different requirements for KITL in proliferation and migration of mouse primordial germ cells. Biol Reprod 2005;73:639–647. [PubMed: 15917341]

McMahon JA, Takada S, Zimmerman LB, Fan CM, Harland RM, McMahon AP. Noggin-mediated antagonism of BMP signaling is required for growth and patterning of the neural tube and somite. Genes Dev 1998;12:1438–1452. [PubMed: 9585504]

Mishina Y, Hanks MC, Miura S, Tallquist MD, Behringer RR. Generation of Bmpr/Alk3 conditional knock out mice. Genesis 2002;32:69–72. [PubMed: 11857780]

Mishina Y, Suzuki A, Ueno N, Behringer RR. Bmpr encodes a type I bone morphogenetic protein receptor that is essential for gastrulation during mouse embryogenesis. Genes Dev 1995;9:3027–3037. [PubMed: 8543149]

Molyneaux KA, Stallock J, Schaible K, Wylie C. Time-lapse analysis of living mouse germ cell migration. Dev Biol 2001;240:488–498. [PubMed: 11784078]

Molyneaux KA, Wang Y, Schaible K, Wylie C. Transcriptional profiling identifies genes differentially expressed during and after migration in murine primordial germ cells. Gene Expr Patterns 2004;4:167–181. [PubMed: 15161097]

Molyneaux KA, Zinszner H, Kunwar PS, Schaible K, Stebler J, Sunshine MJ, O'Brien W, Raz E, Littman D, Wylie C, Lehmann R. The chemokine SDF1/CXCL12 and its receptor CXCR4 regulate mouse germ cell migration and survival. Development 2003;130:4279–4286. [PubMed: 12900445]

Monteiro RM, de Sousa Lopes SM, Korchynskyi O, ten Dijke P, Mummery CL. Spatio-temporal activation of Smad1 and Smad5 in vivo: monitoring transcriptional activity of Smad proteins. J Cell Sci 2004;117:4653–4663. [PubMed: 15331632]

Moon AM, Boulet AM, Capecchi MR. Normal limb development in conditional mutants of Fgf4. Development 2000;127:989–996. [PubMed: 10662638]

Obara-Ishihara T, Kuhlman J, Niswander L, Herzlinger D. The surface ectoderm is essential for nephric duct formation in intermediate mesoderm. Development 1999;126:1103–1108. [PubMed: 10021330]

Ohinata Y, Ohta H, Shigeta M, Yamanaka K, Wakayama T, Saitou M. A signaling principle for the specification of the germ cell lineage in mice. Cell 2009;137:571–584. [PubMed: 19410550]

Ohyama T, Groves AK. Generation of Pax2-Cre mice by modification of a Pax2 bacterial artificial chromosome. Genesis 2004;38:195–199. [PubMed: 15083520]

Otsuka F, Shimasaki S. A negative feedback system between oocyte bone morphogenetic protein 15 and granulosa cell kit ligand: its role in regulating granulosa cell mitosis. Proc Natl Acad Sci U S A 2002;99:8060–8865. [PubMed: 12048244]

Ross A, Munger S, Capel B. Bmp7 regulates germ cell proliferation in mouse fetal gonads. Sex Dev 2007;1:127–137. [PubMed: 18391523]

Runyan C, Schaible K, Molyneaux K, Wang Z, Levin L, Wylie C. Steel factor controls midline cell death of primordial germ cells and is essential for their normal proliferation and migration. Development 2006;133:4861–4869. [PubMed: 17107997]

Russell ES. Hereditary anemias of the mouse: a review for geneticists. Adv Genet 1979;20:357–459. [PubMed: 390999]

Saitou M, Barton SC, Surani MA. A molecular programme for the specification of germ cell fate in mice. Nature 2002;418:293–300. [PubMed: 12124616]

Solloway MJ, Robertson EJ. Early embryonic lethality in Bmp5;Bmp7 double mutant mice suggests functional redundancy within the 60A subgroup. Development 1999;126:1753–1768. [PubMed: 10079236]

Soriano P. Generalized lacZ expression with the ROSA26 Cre reporter strain. Nat Genet 1999;21:70–71. [PubMed: 9916792]

Stebler J, Spieler D, Slanchev K, Molyneaux KA, Richter U, Cojocaru V, Tarabykin V, Wylie C, Kessel M, Raz E. Primordial germ cell migration in the chick and mouse embryo: the role of the chemokine SDF-1/CXCL12. Dev Biol 2004;272:351–361. [PubMed: 15282153]

ten Dijke P, Korchynskyi O, Valdimarsdottir G, Goumans MJ. Controlling cell fate by bone morphogenetic protein receptors. Mol Cell Endocrinol 2003;211:105–113. [PubMed: 14656483]

Valdimarsdottir G, Goumans MJ, Rosendahl A, Brugman M, Itoh S, Lebrin F, Sideras P, ten Dijke P. Stimulation of Id1 expression by bone morphogenetic protein is sufficient and necessary for bone

morphogenetic protein-induced activation of endothelial cells. Circulation 2002;106:2263–2270. [PubMed: 12390958]

Wang GJ, Brenner-Anantharam A, Vaughan ED, Herzlinger D. Antagonism of BMP4 signaling disrupts smooth muscle investment of the ureter and ureteropelvic junction. J Urol 2009;181:401–407. [PubMed: 19010499]

Wehrle-Haller B, Weston JA. Soluble and cell-bound forms of steel factor activity play distinct roles in melanocyte precursor dispersal and survival on the lateral neural crest migration pathway. Development 1995;121:731–742. [PubMed: 7536655]

Wei W, Qing T, Ye X, Liu H, Zhang D, Yang W, Deng H. Primordial germ cell specification from embryonic stem cells. PLoS One 2008;3:e4013. [PubMed: 19107197]

Weidinger G, Wolke U, Koprunner M, Thisse C, Thisse B, Raz E. Regulation of zebrafish primordial germ cell migration by attraction towards an intermediate target. Development 2002;129:25–36. [PubMed: 11782398]

Winnier G, Blessing M, Labosky PA, Hogan BL. Bone morphogenetic protein-4 is required for mesoderm formation and patterning in the mouse. Genes Dev 1995;9:2105–2116. [PubMed: 7657163]

Xu PX, Zheng W, Huang L, Maire P, Laclef C, Silvius D. Six1 is required for the early organogenesis of mammalian kidney. Development 2003;130:3085–3094. [PubMed: 12783782]

Ying Y, Qi X, Zhao GQ. Induction of primordial germ cells from murine epiblasts by synergistic action of BMP4 and BMP8B signaling pathways. Proc Natl Acad Sci U S A 2001;98:7858–7862. [PubMed: 11427739]

Ying Y, Zhao GQ. Cooperation of endoderm-derived BMP2 and extraembryonic ectoderm-derived BMP4 in primordial germ cell generation in the mouse. Dev Biol 2001;232:484–492. [PubMed: 11401407]

Zakin L, Reversade B, Kuroda H, Lyons KM, De Robertis EM. Sirenomelia in Bmp7 and Tsg compound mutant mice: requirement for Bmp signaling in the development of ventral posterior mesoderm. Development 2005;132:2489–2499. [PubMed: 15843411]

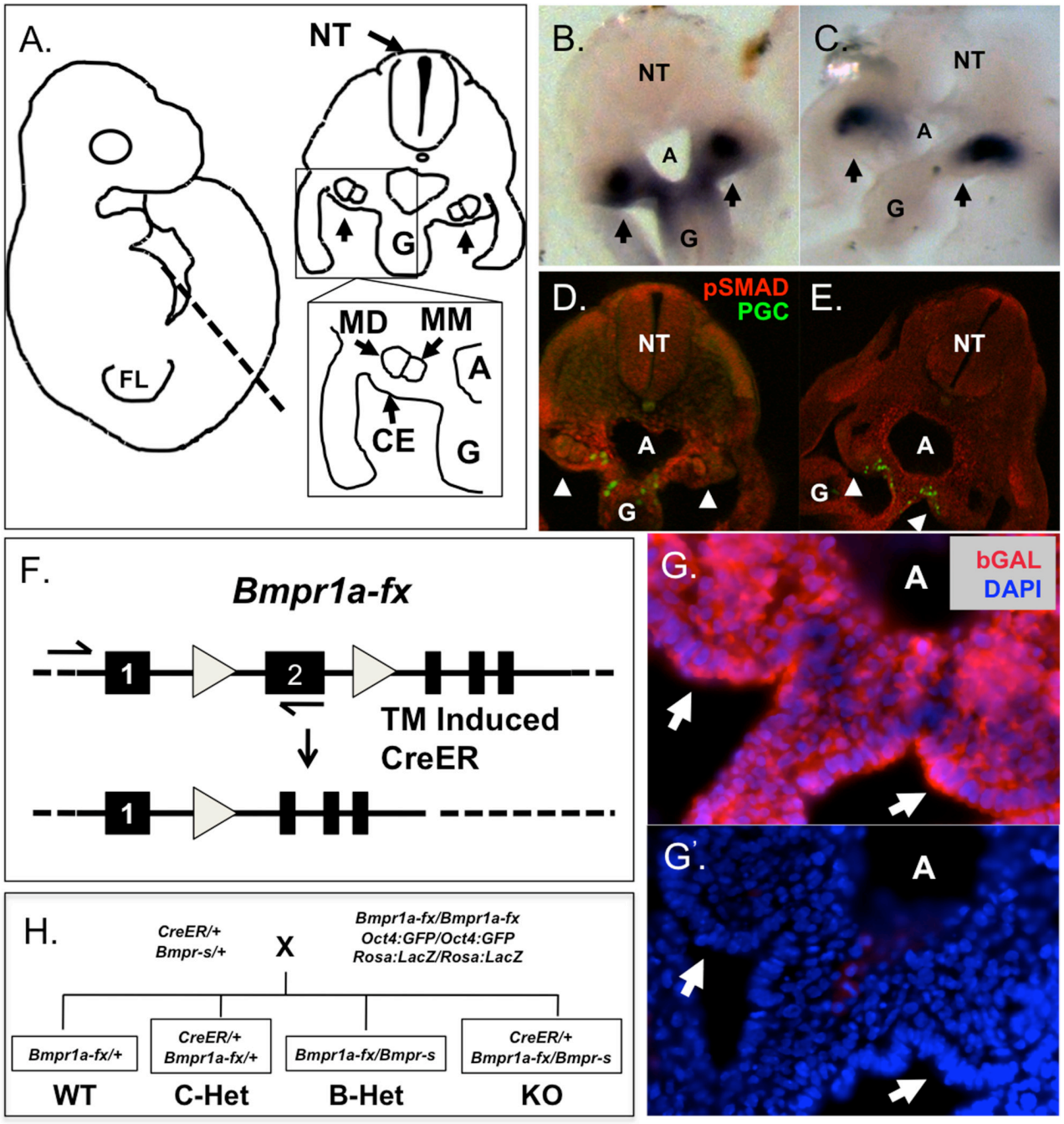

Figure 1.

Tools for targeting BMP-signaling during PGC migration. (A) Transverse tissue sections containing PGCs were isolated as shown. This cartoon illustrates the morphology of a typical slice taken at E9.5. Slices may be larger or smaller based on their position along the AP axis. (B, C) In situ hybridization of E9.5 tissue with probes for *Bmp 4* (B) and *Bmp7 (C). Bmp4* is expressed in mesenchymal cells along the PGC migration route. In the genital ridge, *Bmp7* expression is limited to the mesonephric duct (D, E). Immunostaining for phosphorylated SMAD1/5/8 (pSMAD1/5/8) reveals BMP-responsive cells at (D) E9.5 and (E) E10.5. (F) Cre-LoxP strategy used to target *Bmpr1a*. (G, G') Excision efficiency was tested using the *Rosa:LacZ* reporter. CreER/+ mice were crossed to mice homozygous for the *Rosa:LacZ*

reporter. Tamoxifen was administered at E8.5 and recombination assayed by immunostaining at E10.5. β-gal expression (red) is seen in *CreER/+*, *Rosa:LacZ/+* embryos (G) but not in *Rosa:LacZ/+* sibling controls (G'). DAPI is shown as blue. (H) Breeding strategy to generate a tamoxifen inducible loss of *Bmpr1a*. Four genotypes of offspring are possible. In KO and C-Het embryos, tamoxifen will induce recombination of the *Bmpr1a-fx* allele. *Bmpr-s* is a null allele of *Bmpr1a*. FL = fore-limb bud, NT = neural tube, MM = mesonephric mesenchyme, MD = mesonephric duct, CE = coelomic epithelium, A = aorta, G = gut, PGC = primordial germ cells. Arrows indicate the genital ridges.

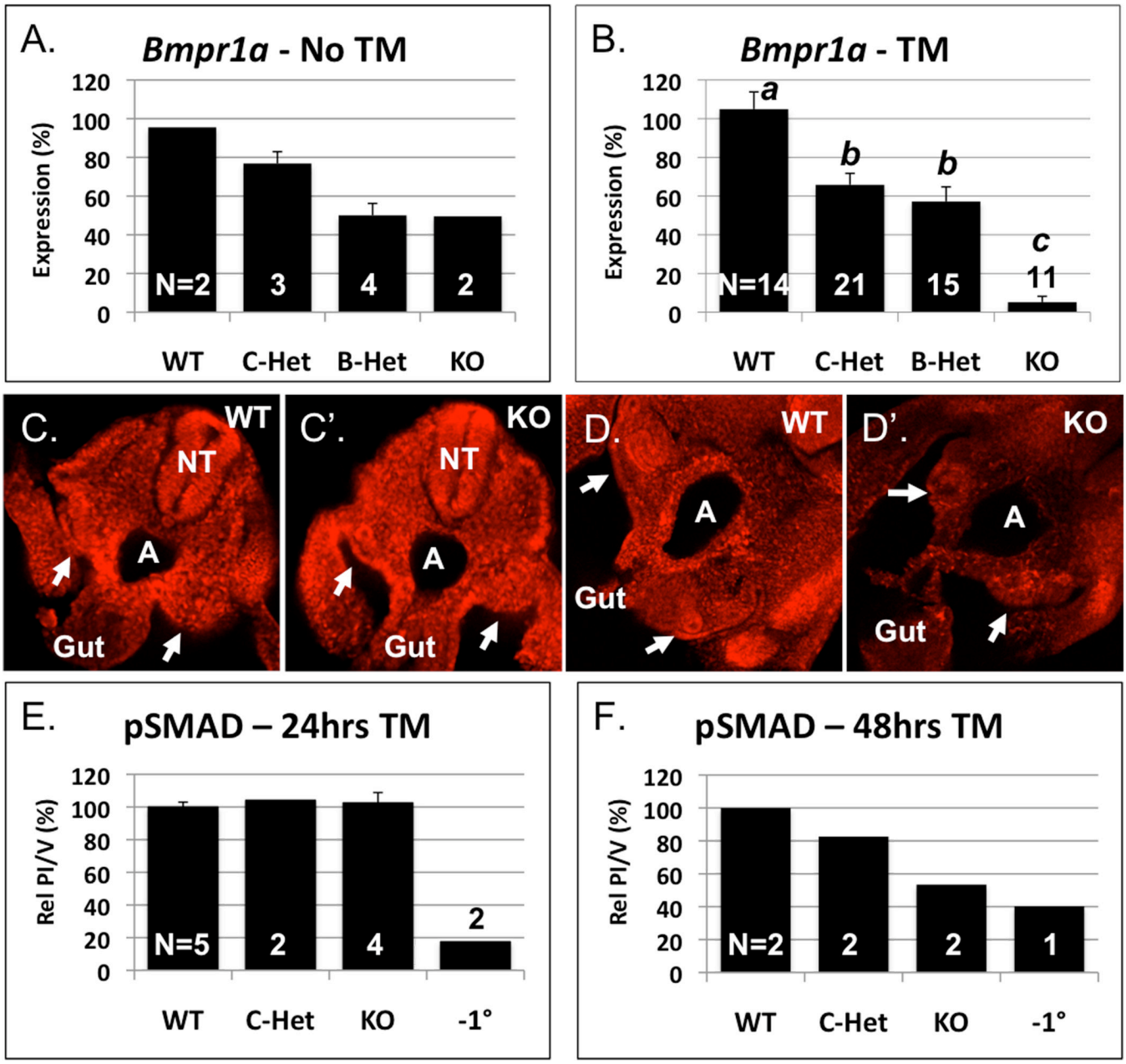

Figure 2.

Tamoxifen induced Cre recombination of *Bmpr1a-fx* leads to decreased expression of *Bmpr1a* and decreased BMP signaling. q-RT-PCR was used to monitor the level of *Bmpr1a* mRNA in E10.5 tissue slices taken between the fore- and hind-limb buds. E10.5 KO embryos that had not been exposed to tamoxifen had *Bmpr1a* mRNA levels similar to their B-Het siblings (A). KO embryos treated with TM at E8.5 and harvested at E10.5 had reduced *Bmpr1a* levels (B). Immunostaining for pSMAD1/5/8 was used to monitor BMP signaling in WT (C, D) and KO (C', D') TM-treated embryos at E9.5 (C, C') and E10.5 (D, D'). Staining intensity (relative pixel intensity per μm^3) was quantified at E9.5 (E) and E10.5 (F) using Volocity software. Expression and pSMAD staining data were compared between the different genotypes using one-way ANOVA followed by the Fisher's least significant difference post test. Data sets that were deemed equivalent are marked with the same letter (*a–c*). Arrows mark

the genital ridges. TM = tamoxifen, A = aorta, NT = neural tube, −1° = no primary antibody, N = number of embryos. Error bars are standard error of the mean (s.e.m.).

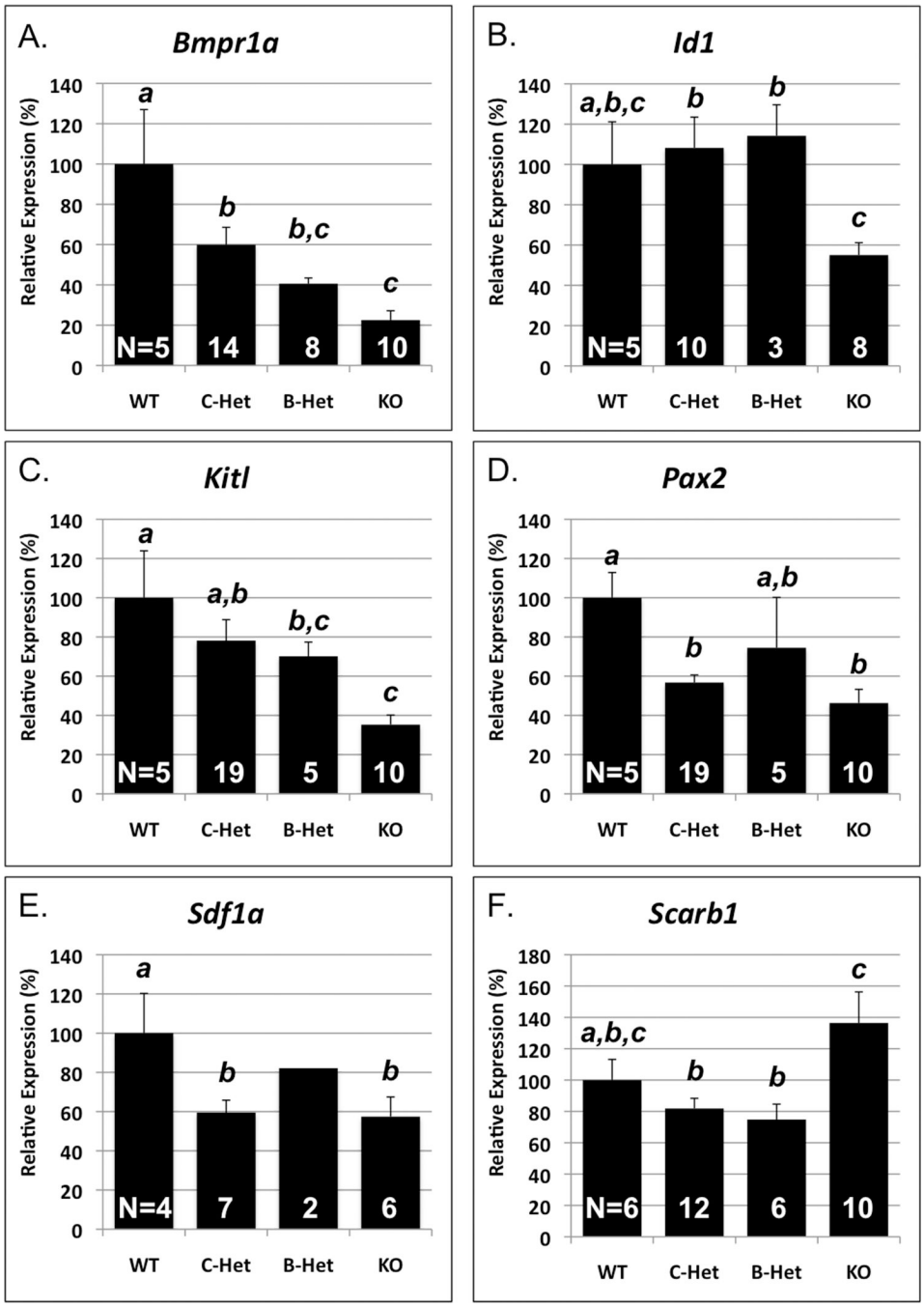

Figure 3.

Expression of BMP target genes are reduced in the genital ridges of *Bmpr1a* conditional knock out embryos. TM was administered at E8.5 and embryos were harvested at E10.5. Tissue slices were dissected and the genital ridges were further dissected away from the neural tube and gut. q-RT-PCR was used to measure the expression of *Bmpr1a* (A), known and putative BMP target genes *Id1* (B), *Kitl* (C), *Pax2* (D), and *Sdf1a* (E), and the epithelial marker gene *Scarb1* (F). Results were significant by ANOVA followed by Fisher's least significance testing as indicated (lower case letters), $F<0.05$. WT = wild type, C-Het = conditional heterozygote, B-Het = *Bmpr-s* heterozygote, KO = knock out, N = number of embryos. Error bars are s.e.m.

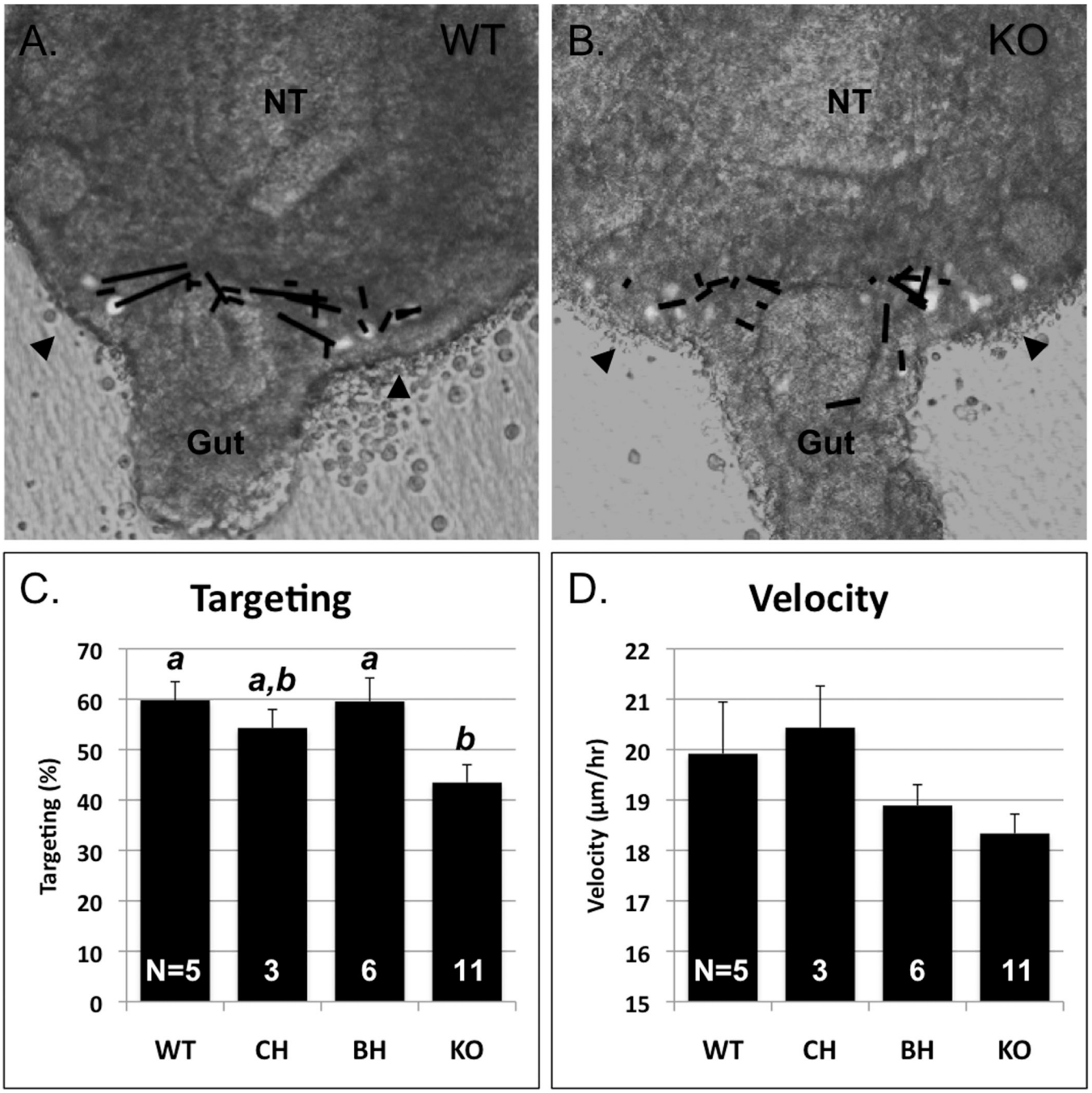

Figure 4.

Conditional loss of *Bmpr1a* leads to reduced PGC targeting of genital ridges. Tamoxifen was administered at E8.5 and embryos harvested at E9.5. Transverse sections were then cultured on the stage of a confocal microscope and time-lapse images collected every 7 minutes for 100 frames. Volocity software was used to track the trajectories of the PGCs in wild type (A, black lines, Movie 1) and knock out tissue (B, black lines, Movie 2). PGCs were then scored as either targeting the genital ridges (A, B, arrowheads) or migrating away from the nearest ridge, revealing decreased targeting in KO tissue significant by ANOVA followed by Fisher's least significant difference test, F = 0.01 (C). Additionally there was a slight but not significant decrease in PGC velocity in KO tissue relative to the wild type (D). PGCs express the GFP

marker and arrows mark genital ridges. NT = neural tube, N = number of embryos. Error bars are s.e.m.

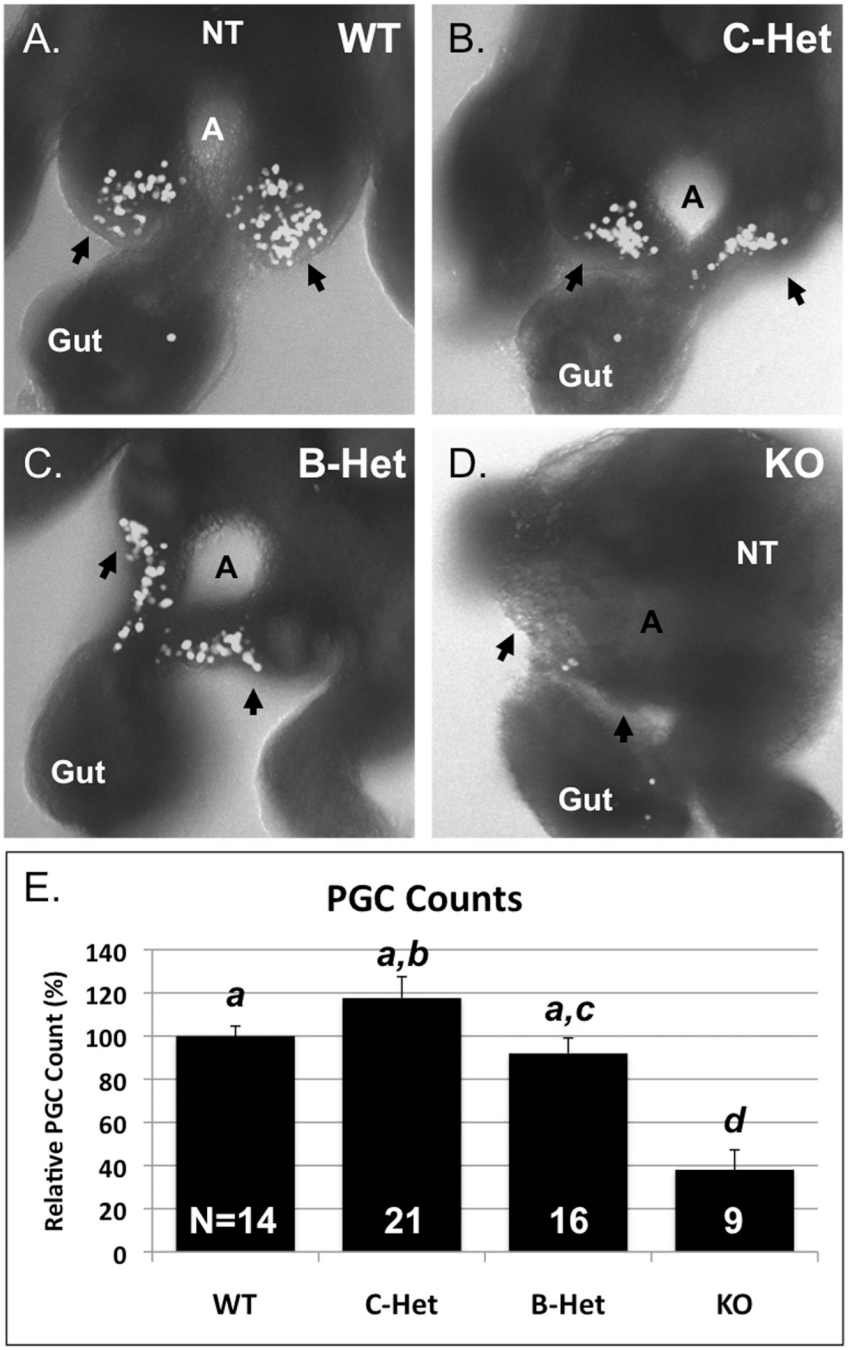

Figure 5.

Reduced BMP signaling leads to decreased numbers of PGCs in vivo. Representative transverse sections of E10.5 wild type (A), C-Het (B), B-Het (C), and KO (D) embryos show the abundance and location of PGCs (GFP positive). Counts of PGCs in E10.5 WT, C-Het, B-Het, and KO embryos showed that there are significantly fewer PGCs in KO embryos relative to their wild type and heterozygous littermates (E). Results are significant by ANOVA followed by Fisher's least significant differences test, F = 0.000004. Arrowheads mark genital ridges. A = aorta, NT = neural tube, N = number of embryos. Error bars are s.e.m.

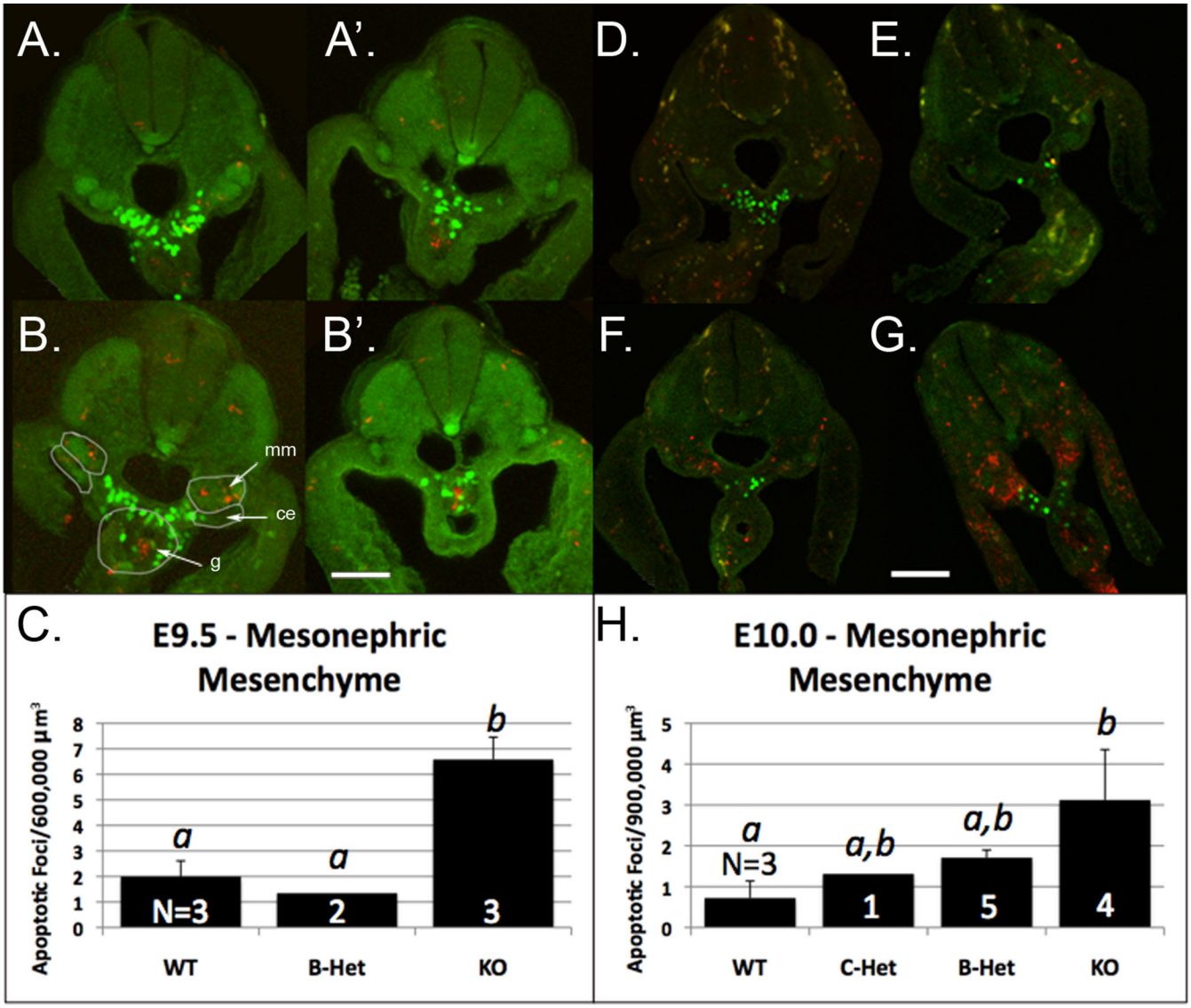

Figure 6.

Conditional loss of *Bmpr1a* leads to increased somatic cell apoptosis in the mesonephric mesenchyme. Immunostaining for cleaved PARP (red) in an anterior slice taken from a WT E9.5 embryo (A) and a more posterior slice taken from the same embryo (A'). cPARP staining in an anterior slice taken from a KO E9.5 embryo (B) and a more posterior slice taken from the same embryo (B'). The mutant has more cell death within the anterior mesonephric mesenchyme than the wildtype. More posterior positions are less effected (B'). Examples of the regions selected for counting cPARP foci are circled in (B). For each slice, Volocity software was used to count the number of apoptotic foci in the mesonephric mesenchyme (mm) (C), coelomic epithelium (ce), and gut (g) (data not shown). Examples of cPARP staining at E10.0 in WT (D), B-Het (E), and KO (F, G) tissue slices. KO embryos have either a modest increase in cell death (F) or in rare cases a dramatic increase in cell death (G) in the mesonephric mesenchyme. cPARP foci were counted as described above and the amount of cell death in the mesonephric mesenchyme is displayed (H). E10.0 samples with extreme cell death (G) were not used for quantitation because it was not possible to count individual foci accurately. There were significantly more apoptotic foci in the KO mesonephric mesenchyme than in the

WT at both E9.5 (C) and E10.0 (H). Results are significant by ANOVA followed by Fisher's least significant difference test, F = 0.000004 (C) and F = 0.039 (H). PGCs express the GFP marker. Scale bars: 100 μm (A – B'), and 160 μm (D–G). Error bars are s.e.m.